GEOMETRIC INTERPRETATION OF MULTIACCESS JOINT DETECTION AND THE ALTERNATING PROJECTION ALGORITHM

Rachel E. Learned Stephane Mallat Bernhard Claus Alan S. Willsky

Laboratory for Information and Decision Systems
Massachusetts Institute of Technology
December 20, 1994

This paper, with the exception of Section 8 (examples), appears in ICASSP-95

ABSTRACT

The joint detection of all users in a multiple access (MA) communication system in which user transmissions are correlated has been shown in recent literature to enhance the system performance relative to that achieved without joint detection. Over the past several years the area of low complexity joint detectors has received much attention. This paper explains the problem of multiple access joint detection in geometrical terms. Geometric interpretation leads to the proposal of an alternating projection joint detection algorithm (APJD). Due to some similarities between our APJD and the multistage joint detector (MJD) of Varansi and Aazhang [5], the MJD is also discussed. The APJD is guaranteed to converge and a proof is given. The geometric interpretation of the MA joint detection problem allows for the exploration of determining, a priori, the error probability of a joint detector and user waveform set in the absence of noise. Simulations offer empirical characterization of the error behavior of both detectors.

1. MULTIPLE ACCESS COMMUNICATION AND DETECTION

A multiple access (MA) communication system will typically support a large number of users over a given channel. Many users are allowed to transmit simultaneously in the same frequency band; each user transmits a single bit by modulating a pre-assigned signature waveform by a +1 or -1. The common MA scenario used for this paper is that of synchronous signaling through the additive white Gaussian noise channel with no intersymbol interference. With no loss of generality, we may focus our attention to one bit duration, i.e. within a single block of time all users transmit a single bit.

Assign the k^{th} user a signature waveform, $s_k(t)$, which is zero outside of an interval I. Assume that the set of user waveforms span a signal space, $span\{s_k(t)\} \subset L^2(I)$, of dimension N. Choosing an orthonormal basis of $span\{s_k(t)\}$ allows for us to represent each user signature as $\mathbf{s}_k$, the N-dimensional column vector of coefficients (with respect to their basis) corresponding to $s_k(t)$. Note that $span\{\mathbf{s}_k\} = I\!R^N$. Let the k^{th} user's bit be denoted by $b_k \in \{+1, -1\}$, where each value occurs with equal probability. The received signal is then represented as a coefficient vector, $\mathbf{r}$,

$$\mathbf{r} = \sum_{k=1}^{K} b_k \mathbf{s}_k + \mathbf{n} = \mathbf{S}^T \mathbf{b} + \mathbf{n} \tag{1}$$

where K is the total number of users, $\mathbf{n}$ is the coefficient vector of noise[1], $\mathbf{b} \triangleq [b_1\ b_2 \cdots b_K]^T$ and $\mathbf{S}^T \triangleq [\mathbf{s}_1\ \mathbf{s}_2 \cdots \mathbf{s}_K]$.

The conventional approach to receiver design is to use a matched filter and slicer,

$$\hat{b}_k = \mathrm{sgn}[\mathbf{r}^T \mathbf{s}_k], \tag{2}$$

where sgn represents the signum function and $\hat{b}_k$ denotes the estimated/detected bit of the k^{th} user. The conventional matched filter (2) represents the optimal receiver in the case where the MAI is assumed normal and white. Under this assumption, as users are added to the system the MAI raises the noise level; this, in turn, limits the matched filter performance.

The MAI, however, is not an additive white Gaussian noise process; it possesses a great degree of structure which can be exploited in building receivers which have better performance than the conventional detector. The optimal joint detector (which accounts for the MAI) maximizes the log-likelihood function [7] and results in

$$\hat{\mathbf{b}} = \arg\left[\max_{\mathbf{b} \in \{1,-1\}^K} 2\mathbf{r}^T \mathbf{S}^T \mathbf{b} - (\mathbf{S}^T \mathbf{b})^T \mathbf{S}^T \mathbf{b} \right]. \tag{3}$$

This maximization is over 2^K possible $\mathbf{b}$ vectors (a computational complexity that is exponential in K, the number of users). This optimal method offers substantially higher performance than the conventional demodulator (2), but is of little practical use on account of its computational burden [4].

The work of S. Mallat was supported by the AFOSR grant F49620-93-1-0102, ONR grant N00014-91-J-1967. The work of the other authors has been supported in part by the National Science Foundation under grant number MIP-9015281 and by the Air Force Office of Scientific Research under grant number F49620-92-J-0002.

[1] The irrelevance theorem allows for the portion of the noise which lies outside of $span\{s_k(t)\}$ to be ignored [9] .

Recent communication literature addresses the general notion of *suboptimal* joint detection which offers computational improvement relative to the optimal method while achieving a significant improvement in performance over the conventional detector. The state of the art is reviewed in the paper by Verdu [8]. In particular, one approach that has been shown to offer good performance compared to other methods is the multistage joint detector (MJD) developed by Varanasi and Aazhang in [5] and [6]. The MJD corresponding to the received signal vector of Equation (1) is

$$\hat{\mathbf{b}}(m+1) = \text{sgn}[\mathbf{Sr} + (\mathbf{E} - \mathbf{SS}^T)\hat{\mathbf{b}}(m)], \tag{4}$$

where the energy matrix $\mathbf{E} \triangleq \text{diag}\ (< \mathbf{s}_k, \mathbf{s}_k >)_{k=1}^K$. The MJD is motivated by separating Equation (1) in the noiseless case (for each user k) into two parts, the MAI and the signal of interest, and then applying the appropriate matched filter for user k to yield

$$\mathbf{s}_k^T\mathbf{r} = \sum_{i \neq k} b_i \mathbf{s}_k^T \mathbf{s}_i + b_k \mathbf{s}_k^T \mathbf{s}_k. \tag{5}$$

After rearranging and rewriting Equation (5) for all users in vector form, we obtain

$$\mathbf{Eb} = \mathbf{Sr} + (\mathbf{E} - \mathbf{SS}^T)\mathbf{b}, \tag{6}$$

the impetus for the MJD. The MJD estimates the MAI and subtracts it from the output of the bank of matched filters to obtain an estimate of the desired bit. This process is iterated to obtain "better" estimates of the MAI in the hope of improving the estimate of the desired bit.

The problem of finding the correct bit vector from the aggregate can be shown to be N-P complete.[2] Primarily, there is the problem of heuristic approaches converging to local minima. MA joint detection, therefore, is not going to be solved by a simple trick.

This paper looks at the problem in geometrical terms in Section 2, revealing its structure. The structure is reminiscent of other problems which are solved via alternating projections. An appropriate alternating projection joint detector (APJD) is deduced and shown to converge in Section 3. The MJD, viewed as a sequence of operators within our geometry and can easily be shown (in some cases) to loop between two incorrect bit vector estimates. The differences between the MJD the APJD are discussed in Section 4. The geometric framework allows for us to begin the characterization of errors for suboptimal joint detectors. This idea is briefly discussed for the APJD and MJD and an empirical examination of the errors is done via simulations for both the APJD and the MJD in Section 5. The paper is concluded in Section 6.

2. GEOMETRICAL PRESENTATION OF THE MA DETECTION PROBLEM

In order to examine the MJD and develop an appropriate low complexity joint detection algorithm the detection problem is described in a geometrical framework. To begin our understanding of the problem we examine its fundamental structure in the absence of noise. For the remainder of this paper, noise is omitted.

Define the set of bit vectors

$$\Gamma \triangleq \{[b_1 \cdots b_K]^\mathsf{T} \mid b_i \in \{+1, -1\}\ \forall i = 1, \cdots, K\}.$$

Geometrically, Γ comprises the vertices of a hypercube of dimension K. For $K > N$ the N-dimensional signature vectors, $\{\mathbf{s}_k\}_1^K$, are linearly dependent.[3] This means that the solution, $\mathbf{x}$, to

$$\mathbf{r} = \mathbf{S}^T\mathbf{x} \tag{7}$$

is not unique. By definition of linear dependence, we have

$$\mathbf{S}^T\alpha = 0 \tag{8}$$

for any $\alpha \in \mathcal{N}(\mathbf{S}^T)$, the nullspace of $\mathbf{S}^T$. We may, then, express the solution of Equation (7) as

$$\mathbf{x} = \beta + \alpha, \tag{9}$$

where β is the solution of Equation (7) for which $\beta \perp \alpha$. The only solutions of interest to the MA problem stated in this paper are contained in the set Γ. For every $\beta \perp \mathcal{N}(\mathbf{S}^T)$ which solves Equation (7) we are interested only in the solutions for which $(\beta + \alpha) \in \Gamma$, where $\alpha \in \mathcal{N}(\mathbf{S}^T)$.

A geometric interpretation of the above discussion follows. We have our set of possible solutions, Γ, the vertices of a K-dimensional hypercube. We separate our solution, $\mathbf{x}$, into two parts, α and β. This corresponds to viewing our vector space, $\mathbb{R}^K$, as the Cartesian product of two subspaces, $\mathcal{N}(\mathbf{S}^T)$ and the space which is orthogonal to $\mathcal{N}(\mathbf{S}^T)$. Given the uniquely determined solution, $\beta \perp \mathcal{N}(\mathbf{S}^T)$, the general solution must lie in the affine space $\mathcal{W} \triangleq \mathcal{N}(\mathbf{S}^T) + \beta$. The MA joint detection problem corresponds, geometrically, to finding the point, $\mathbf{x}$, which lies in the intersection of the set Γ and the affine space $\mathcal{W}$.

The definition of β may be specified further. The set of user signature waveform vectors, $\{\mathbf{s}_k\}_1^K$, comprise a frame for the space $span\{\mathbf{s}_k\}$.[4] Let $\{\tilde{\mathbf{s}}_k\}_1^K$ be the corresponding dual frame, defined via the dual frame operator

$$\tilde{\mathbf{S}} \triangleq [\tilde{\mathbf{s}}_1\ \tilde{\mathbf{s}}_2 \cdots \tilde{\mathbf{s}}_K] = \mathbf{S}(\mathbf{S}^T\mathbf{S})^{-1}.$$

We may decompose $\mathbf{r}$ using the dual frame operator

$$< \tilde{\mathbf{s}}_k, \mathbf{r} >= \tilde{\mathbf{S}}\mathbf{r}, \tag{10}$$

and we may reconstruct using the frame reconstruction formula

$$\mathbf{r} = \sum_{k=1}^{K} < \mathbf{r}, \tilde{\mathbf{s}}_k > \mathbf{s}_k = \mathbf{S}^T\tilde{\mathbf{S}}\mathbf{r}\ . \tag{11}$$

Note the similarities between Equation (11) and the MA aggregate signal of Equation (1). Since $\tilde{\mathbf{S}}r$ has the same

[2] This issue is examined by Verdu in [4].

[3] This is the case in which the number of users is greater than the dimension of the span of their signature waveforms.

[4] For our purposes it is sufficient to note that a subset of the signature waveforms $\{\mathbf{s}_k\}$ constitute a basis of the considered space and that no $\mathbf{s}_k$ is identically zero. See the text by Daubechies for a tutorial treatment of frame theory [1].

properties that were required of β: $\tilde{\mathbf{S}}r \in \mathcal{R}(\tilde{\mathbf{S}}) = \mathcal{R}(\mathbf{S})$[5] and $\mathcal{R}(\mathbf{S}) \perp \mathcal{N}(\mathbf{S}^T)$ [6], we see that the frame reconstruction Equation (11) corresponds to the unique portion of the solution of our MA joint detection problem, thus, $\beta = \tilde{\mathbf{S}}\mathbf{r}$.

3. THE ALTERNATING PROJECTION JOINT DETECTOR

As discussed in Section 2 the MA joint detection problem reduces to finding the point

$$\hat{\mathbf{b}} \in \Gamma \cap \mathcal{W}.$$

The problem of finding the intersection between two convex sets is known to be solved iteratively by alternating projections between the two sets. Our problem differs from this in that one of our sets, Γ, is not convex. Noting the similarities between the two problems, we propose the alternating projection approach for the MA joint detection problem and prove convergence.

Theorem: We define two projection operators; $\mathbf{P}_\Gamma$ maps a vector in $\mathbb{R}^K$ to the closest vector in Γ, and $\mathbf{P}_\mathcal{W}$ maps a vector in $\mathbb{R}^K$ to the closest vector in $\mathcal{W}$. By closest, we mean shortest Euclidean distance.[7] Thus, the following alternating projection joint detector (APJD) is guaranteed to converge in a finite number of steps.

$$\hat{\mathbf{b}}(m+1) = \mathbf{P}_\Gamma \mathbf{P}_\mathcal{W} \hat{\mathbf{b}}(m) \tag{12}$$

Proof: Let $d(\mathbf{x}, \mathbf{y})$ denote the Euclidean distance between the two vectors $\mathbf{x}$ and $\mathbf{y}$. For guaranteed convergence we need to show that

$$d(\hat{\mathbf{b}}(m+1), \mathbf{P}_\mathcal{W}\hat{\mathbf{b}}(m+1)) \leq d(\hat{\mathbf{b}}(m), \mathbf{P}_\mathcal{W}\hat{\mathbf{b}}(m)),$$

where the equality holds only for $\hat{\mathbf{b}}(m+1) = \hat{\mathbf{b}}(m)$. In words, we wish to show that with every iteration of the APJD, the estimate gets closer to the affine space $\mathcal{W}$.

We assert the following:

$$\begin{aligned} d(\hat{\mathbf{b}}(m+1), \mathbf{P}_\mathcal{W}\hat{\mathbf{b}}(m+1)) &\leq d(\hat{\mathbf{b}}(m+1), \mathbf{P}_\mathcal{W}\hat{\mathbf{b}}(m)) \\ &\leq d(\hat{\mathbf{b}}(m), \mathbf{P}_\mathcal{W}\hat{\mathbf{b}}(m)). \end{aligned}$$

The validity of the above equation is explained. The left comparison: by definition of $\mathbf{P}_\mathcal{W}$, we know that $\hat{\mathbf{b}}(m+1)$ is closer to $\mathbf{P}_\mathcal{W}\hat{\mathbf{b}}(m+1)$ than it is to $\mathbf{P}_\mathcal{W}\hat{\mathbf{b}}(m)$ with equality only in the case $\mathbf{P}_\mathcal{W}\hat{\mathbf{b}}(m+1) = \mathbf{P}_\mathcal{W}\hat{\mathbf{b}}(m)$. The right comparison: by the construction of $\hat{\mathbf{b}}(m+1)$ from Equation (12) and from definition of $\mathbf{P}_\Gamma$, we know that $\mathbf{P}_\mathcal{W}\hat{\mathbf{b}}(m)$ is closer to $\hat{\mathbf{b}}(m+1)$ than it is to $\hat{\mathbf{b}}(m)$ with equality only in the case when the points are the same, $\hat{\mathbf{b}}(m+1) = \hat{\mathbf{b}}(m)$. We have equality in both comparisons if and only if $\mathbf{P}_\mathcal{W}\hat{\mathbf{b}}(m+1) = \mathbf{P}_\mathcal{W}\hat{\mathbf{b}}(m)$ *and* the points are the same. Since there are a finite number of points in Γ, the algorithm is guaranteed to converge in a finite number of steps. □

[5]It is easy to show that $\mathcal{R}(\mathbf{S}) = \mathcal{R}(\tilde{\mathbf{S}})$ but is not proved here.

[6]$\mathcal{R}(\mathbf{S})$ denotes the range of $\mathbf{S}$. For more details on the relations between vector spaces, see the text by Strang [3].

[7]These projectors are not required to be linear, i.e. $\mathbf{P}(\mathbf{a}+\mathbf{b}) \neq \mathbf{P}\mathbf{a} + \mathbf{P}\mathbf{b}$.

Unlike alternating projections between two intersecting convex sets, the APJD is an alternating projection between a convex set, $\mathcal{W}$, and a non-convex set, Γ. In such a situation, the alternating projection procedure may result in a "locally best" solution. By this we mean that the APJD will converge to a point, $\hat{\mathbf{b}} \notin \Gamma \cap \mathcal{W}$, where at each step of the iteration the distance between $\hat{\mathbf{b}}(m)$ and $\mathcal{W}$ decreased, and where $\hat{\mathbf{b}}$ is a fixed point of Equation (12).

Our problem of finding the intersection between $\mathcal{W}$ and Γ can be shown to be N-P complete. No solution which is polynomial in complexity is known to solve the N-P complete problem. Moreover, any approach which is polynomial in complexity will suffer from possible convergence to local minima. With this in mind, we know that there is no low complexity suboptimal joint detection procedure which converges to the solution. Instead, we strive to understand the problem so that joint detection algorithms can be developed in order to minimize the probability of converging to a local minima.

We wish to derive the operators, $\mathbf{P}_\Gamma$ and $\mathbf{P}_\mathcal{W}$. It is easy to see that $\mathbf{P}_\Gamma$ is the sgn function. To find $\mathbf{P}_\mathcal{W}$ we begin with the definition of $\mathcal{W}$

$$\mathcal{W} \triangleq \tilde{\mathbf{S}}\mathbf{r} + \mathcal{N}(\mathbf{S}^T).$$

The projection onto $\mathcal{W}$ is, therefore, the projection onto $\mathcal{N}(\mathbf{S}^T)$ translated by $\tilde{\mathbf{S}}\mathbf{r}$,

$$\mathbf{P}_\mathcal{W}\mathbf{x} = \mathbf{P}_\perp \mathbf{x} + \tilde{\mathbf{S}}\mathbf{r}, \tag{13}$$

where $\mathbf{P}_\perp$ is the projector onto $\mathcal{N}(\mathbf{S}^T)$. Using the identity $\mathbf{P}_\perp = (I - \mathbf{P})$ and the projector[8] $\mathbf{P} = \mathbf{S}(\mathbf{S}^T\mathbf{S})^{-1}\mathbf{S}^T$ we find the APJD in terms of the frame and dual frame operators which define the user signature waveforms

$$\hat{\mathbf{b}}(m+1) = \text{sgn}[\, \tilde{\mathbf{S}}\mathbf{r} + (I - \mathbf{S}(\mathbf{S}^T\mathbf{S})^{-1}\mathbf{S}^T)\hat{\mathbf{b}}(m)]. \tag{14}$$

If we initialize the iteration with $\hat{\mathbf{b}}(0) = \mathbf{0}$ then $\hat{\mathbf{b}}(1) = \mathbf{P}_\Gamma\tilde{\mathbf{S}}\mathbf{r}$.[9]

4. COMPARISON OF APJD AND MJD

A brief comparison of the two detectors is offered. Note the similarities between the APJD of Equation (14) and the MJD of Equation (4). Below are the corresponding components of each detector.

APJD		MJD
decorrelator $\tilde{\mathbf{S}} = \mathbf{S}(\mathbf{S}^T\mathbf{S})^{-1}$	$\leftrightarrow$	matched filter $\mathbf{S}^T$
orthogonal projector $(I - \mathbf{S}(\mathbf{S}^T\mathbf{S})^{-1}\mathbf{S}^T)$	$\leftrightarrow$	linear operator $(\mathbf{E} - \mathbf{S}\mathbf{S}^T)$

The dual frame operator, $\tilde{\mathbf{S}}$, applied to $\mathbf{r}$ gives $\mathbf{S}(\mathbf{S}^T\mathbf{S})^{-1}\mathbf{S}^T\mathbf{b}$, the orthogonal projection of $\mathbf{b}$ onto $\mathcal{R}(\mathbf{S})$ while the matched filter, $\mathbf{S}$, applied to $\mathbf{r}$ gives $\mathbf{S}\mathbf{S}^T\mathbf{b} \in \mathcal{R}(\mathbf{S})$. The orthogonal

[8]The orthogonal projection operator, $\mathbf{P}$ which maps a vector onto the closest point in $\mathcal{R}(\mathbf{A})$ is $\mathbf{P} = \mathbf{A}(\mathbf{A}^T\mathbf{A})^{-1}\mathbf{A}^T$.

[9]This $\hat{\mathbf{b}}(1)$ is the decorrelating linear detector of Lupas and Verdu [2].

projector $(I - \mathbf{S}(\mathbf{S}^T\mathbf{S})^{-1}\mathbf{S}^T)$ applied to $\hat{\mathbf{b}}(m)$ gives an "estimate", $\hat{\alpha} \in \mathcal{N}(\mathbf{S}^T)$, of the true α while the linear operator $(\mathbf{E} - \mathbf{S}\mathbf{S}^T)$ applied to $\hat{\mathbf{b}}(m)$ gives an estimate of the MAI which lies in the space $\mathcal{N}(\mathbf{S}^T) \oplus \mathcal{R}(\mathbf{S})$. Note that the APJD consists of orthogonal projectors while the MJD does not.

The MJD has been found to have limit cycle behavior, i.e. for some correlated waveform sets, the bit vector estimate loops between two incorrect elements of Γ. For lack of space, we leave this topic for another paper.

5. PROBABILITY OF ERROR AND SIMULATION RESULTS

It is expected that these algorithms will fail for a specific set of bit vectors. Viewing the problem and the algorithms geometrically gives the motivation for calculating the error probability of a joint detection algorithm by finding the fraction of "bad" bit vectors for a given set of user waveforms. By "bad" we mean that due to the geometrical relationship between $\mathcal{N}(\mathbf{S}^T)$ and Γ, a subset of Γ will result in incorrect convergence of a joint detection algorithm. We wish to determine the bad points for any given $\mathbf{S}$ and joint detection algorithm. In general, this appears to be a difficult problem and is left for future work.

An empirical study of the "bad" points for a specific class of wavelet packet signature sets is calculated via simulations for the APJD and the MJD. Figure 1 shows the fraction of bit vector errors ("bad" points in Γ) versus number of users. The curve was obtained by running both algorithms for all of the 2^K possible bit vectors for each user signature set (frame). The frames were constructed to be the union of an orthogonal wavelet packet basis roughly corresponding to N FDMA[10] signatures and $(K - N)$ randomly delayed discrete Dirac functions. The number of users ranged from $K = N$ to $K = 2N$ for $N = 4$. As we should expect, from this simple simulation, the fraction of "bad" points increases as K goes from N to $2N$.

The simulation presented here along with others for this type have shown the performance of the APJD to be consistently better than that of the MJD. This performance gap is most likely the result of the MJD using the matched filter while the APJD uses a decorrelating matched filter.[11]

6. CONCLUSION

This paper has presented the MA joint detection problem in geometrical terms, revealing its structure. The structure is reminiscent of other problems which are solved via alternating projections. An appropriate alternating projection joint detector (APJD) was deduced and shown to converge. The similarities between the multistage joint detector (MJD) of Varansi and Aazhang [5] and the APJD were discussed. Since the joint detection problem is N-P complete and does not allow for any heuristic algorithm to converge to the solution, we wish to understand the problem in order to develop joint detection algorithms for which the

[10] Frequency division multiple access waveforms are narrow band orthogonal signals.

[11] Varanasi and Aazhang have shown in [6] that by using the decorrelating matched filter to calculate only the first estimate of the MJD they were able to realize an improvement.

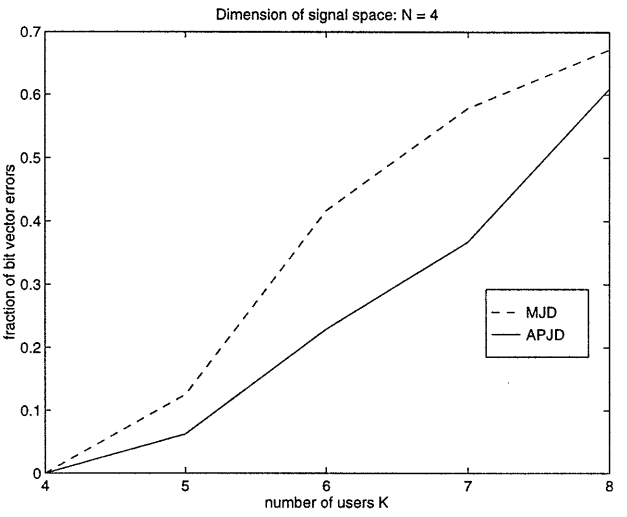

Figure 1: Fraction of incorrect bit vectors ("bad" points) calculated by running the APJD and the MJD with each bit vector in Γ for each frame of the $N = 4$ FDMA-class.

probability of converging to incorrect points in the absence of noise is minimized. Within our geometric framework we anticipate the characterization of errors for joint detectors in general. This appears to be a difficult problem and is left for future work. Via a simple set of simulations for both the APJD and the MJD, we offered a preliminary empirical examination of the behavior of these detectors and the effect of the degree of redundancy in the user waveform sets. As a result of these simulations, the APJD was found to offer better performance over the MJD.

7. REFERENCES

[1] I. Daubechies. *Ten Lectures on Wavelets.* CBMS-NSF, SIAM, Philadelphia, 1992.

[2] R. Lupas and S. Verdu. "Linear multiuser detectors for synchronous code-division multiple-access channels". *IEEE Trans. Inform. Theory*, 35:123–136, Jan. 1989.

[3] G. Strang. *Linear algebra and its applications.* Harcourt Brace Jovanovich, Inc., 1988.

[4] S.Verdu. Computational complexity of optimum multiuser detection. In *Algorithmica.* Springer-Verlag., 1989.

[5] M. Varanasi and B. Aazhang. "Multistage detection in asynchronous code-division multiple-access communications". *IEEE Trans. on Comm.*, 38, Apr. 1990.

[6] M. Varanasi and B. Aazhang. "Optimally near-far resistant multiuser detection in differentially coherent synchronous channels". *IEEE Trans. Inform. Theory*, 37:1006–1018, Jul. 1991.

[7] S. Verdú. "Minimum probability of error for asynchronous gaussian multiple-access channels". *IEEE Trans. Inform. Theory*, 32:85–96, Jan. 1986.

[8] S. Verdú. "Adaptive multiuser detection". In *Third IEEE International Symposium on Spread Spectrum Techniques and Applications*, Oulu, Finland, July 1994.

[9] J.M. Wozencraft and I. M. Jacobs. *"Principles of Communication Engineering"*. J. Wiley, New York, 1965.

8. ADDENDUM: EXAMPLES

Example of the APJD: The APJD algorithm may be examined by "geometrically" walking through the first few iterations of a specific example:

$$\hat{\mathbf{b}}(2) = \mathbf{P}_\Gamma \mathbf{P}_\mathcal{W}(\mathbf{P}_\Gamma \tilde{\mathbf{S}}\mathbf{r}) \tag{15}$$

So that we may display the steps in two dimensions, let the signature waveforms be scalars, $s_1 = 2$, $s_2 = \frac{4}{3}$, and let $b_1 = -1$, $b_2 = 1$, then $\mathbf{S}^T = [2\ \frac{4}{3}]$ and $\mathbf{b} = [-1\ 1]^T$. Figure 2 shows the geometry for this problem. $\mathcal{R}(\mathbf{S})$ is the line through the origin with slope 3/2 and $\mathcal{N}(\mathbf{S}^T)$ is the line through the origin with slope $-2/3$. The set Γ is the vertices of the 2×2 square centered at the origin. The figure shows the result of the application of each projector shown in Equation (15) and is enumerated below. Each intermediate result is denoted by $\mathbf{p}_i$.

1. Dual frame operator, $\tilde{\mathbf{S}}$, applied to $\mathbf{r}$ performs orthogonal projection of $\mathbf{b}$ onto $\mathcal{R}(\mathbf{S})$: $\mathbf{p}_1 = \tilde{\mathbf{S}}\mathbf{r} = \mathbf{S}(\mathbf{S}^T\mathbf{S})^{-1}\mathbf{S}^T\mathbf{b}$
2. Project onto Γ: $\mathbf{p}_2 = \text{sgn}[\mathbf{p}_1]$
3. Project onto $\mathcal{W}$: $\mathbf{p}_3 = \tilde{\mathbf{S}}\mathbf{r} + (I - \mathbf{S}(\mathbf{S}^T\mathbf{S})^{-1}\mathbf{S}^T)\mathbf{p}_2$
4. Project onto Γ: $\mathbf{p}_4 = \text{sgn}[\mathbf{p}_3]$
5. We are back where we were at the end of step 2. The algorithm has converged.

Example of the MJD: The MJD is viewed as a sequence of operators within our geometry and is shown, in this case, to loop between two incorrect bit vector estimates. The MJD is given in Equation (4) and is examined by stepping through the first few iterations:

$$\hat{\mathbf{b}}(3) = \mathbf{P}_\Gamma[\mathbf{S}\mathbf{r} + (\mathbf{E} - \mathbf{S}\mathbf{S}^T)\mathbf{P}_\Gamma[\mathbf{S}\mathbf{r} + (\mathbf{E} - \mathbf{S}\mathbf{S}^T)\hat{\mathbf{b}}(1)]] \tag{16}$$

Initializing $\hat{\mathbf{b}}(0) = \mathbf{0}$, we have $\hat{\mathbf{b}}(1) = \mathbf{P}_\Gamma(\mathbf{S}\mathbf{r})$, the conventional estimates from the output of the bank of matched filters. The same $\mathbf{S}$ and $\mathbf{b}$ used for the last example of the APJD are also used here. Figure 3 and the following steps will lead you through the example.

1. Matched filter the received signal: $\mathbf{p}_1 = \mathbf{S}\mathbf{r} = \mathbf{S}\mathbf{S}^T\mathbf{b}$
2. Project onto Γ: $\mathbf{p}_2 = \mathbf{P}_\Gamma\mathbf{p}_1$
3. Compensate for MAI: $\mathbf{p}_3 = \mathbf{S}\mathbf{r} + (\mathbf{E} - \mathbf{S}\mathbf{S}^T)\mathbf{p}_2$
4. Project onto Γ: $\mathbf{p}_4 = \mathbf{P}_\Gamma\mathbf{p}_3$
5. Compensate for MAI: $\mathbf{p}_5 = \mathbf{S}\mathbf{r} + (\mathbf{E} - \mathbf{S}\mathbf{S}^T)\mathbf{p}_4$
6. Project onto Γ: $\mathbf{p}_6 = \mathbf{P}_\Gamma\mathbf{p}_5$
7. We are back where we were at the end of step 2. The algorithm is confined to a limit cycle.

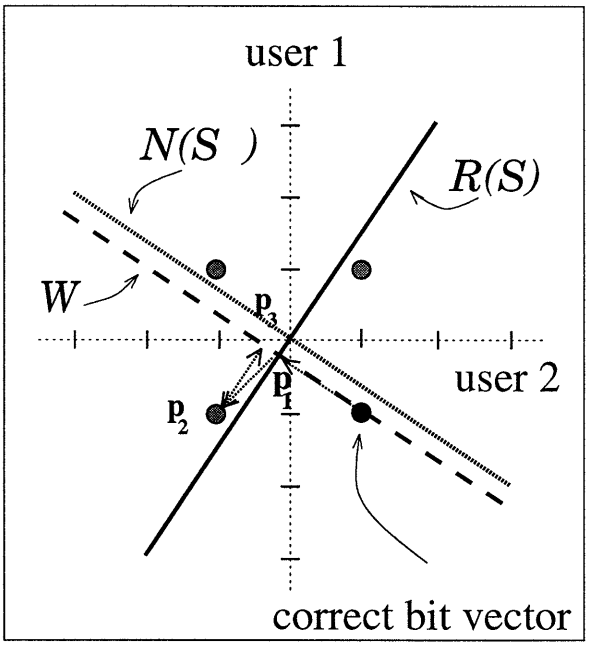

Figure 2: Geometric interpretation of an example of the APJD.

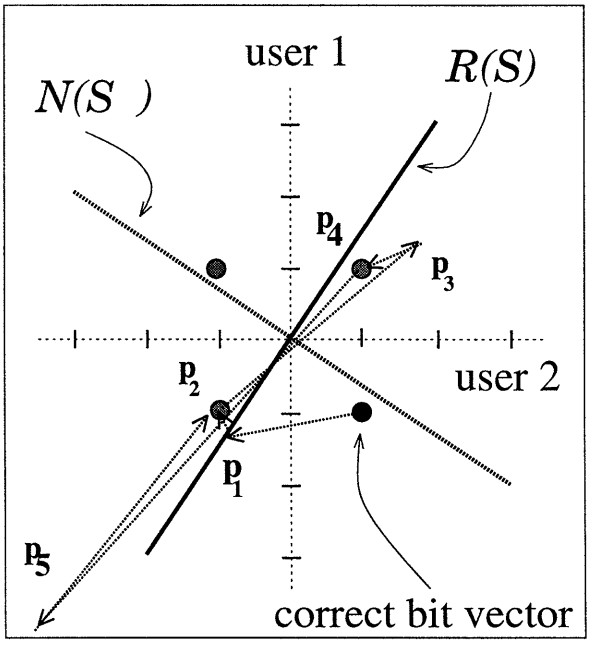

Figure 3: Geometric interpretation of an example of the MJD.